

NUMERICAL STUDY OF ION ORBITS IN THE MAGNETIC PRESHEATHS

P. Lindner, H. Gerhauser and H.A. Claßen

*Institut für Plasmaphysik, Forschungszentrum Jülich GmbH, EURATOM Association
Trilateral Euregio Cluster, D-52425 Jülich, Germany*

1. Introduction

Plasma contamination by impurities is one of the key problems on the way to controlled nuclear fusion. In addition to the impurity ion transport in the plasma, the release of impurity neutrals from the plasma facing components and the penetration depth of the neutrals into the plasma have a significant influence on the plasma contamination, in particular on the central impurity density. The mechanism of impurity release from the walls is determined by the velocity distribution function of the incident ions. Since the reflection and sputtering processes are very sensitive to the distribution of the angle of ion incidence, a careful analysis of this subject is very important, but complicated by the fact that the magnetic field \vec{B} is oblique with respect to most of the intersected wall components. In regions of oblique \vec{B} the plasma-wall transition is characterized by a multiple sheath structure, i.e. by the appearance of a quasineutral magnetic presheath between the Debye sheath in front of the wall and the collisional presheath in the plasma. Inside the magnetic presheath, which very often may be considered as collisionless, the ion gyroorbits are destroyed (the drift approximation ceases to be valid) and the thermal ion gyro-energy is converted into the kinetic energy of the surface-parallel $\vec{E} \times \vec{B}$ motion. The transition from the collisional to the magnetic presheath is defined by the sonic point in the $\|\vec{B}$ velocity of the majority (deuterium background) ion motion. In this paper we calculate the orbits in the magnetic presheath and Debye sheath of at least 10^4 ions representing the velocity distribution of instreaming ions and their ensuing distribution at the wall surface.

2. Numerical Solution of the Equation of Motion for Ions

It is assumed that all quantities depend only on the y-coordinate (see Fig. 1), the wall is in the x-z-plane and completely absorbing, the transport in this region is collisionless, the angle of the magnetic field is $5^\circ \leq \alpha_B \leq 85^\circ$, the potential $\phi(y)$ is determining by the background Deuterium, the impurities have no significant influence on the potential ($n_i \ll n_D$), the electrical field $\vec{E} = -\nabla\phi = -d\phi(y)/dy$ is for $y > l \sim 5c_s/\Omega_i = 5\sqrt{k_B(T_e + T_D)/m_D}/\Omega_D$ negligible. At the sheath entrance $y = l$ the velocity distribution is described by the Maxwellian distribution $f_i(l, \vec{v}) \sim g(v_{\parallel}^2) \exp(-(v_{\parallel} - c_s)^2/v_{th}^2) \exp(-(v_{\perp}^2 + v_x^2)/v_{th}^2)$ which is shifted in v_{\parallel} direction by the Deuterium sound speed c_s . The smoothing factor $g(v_{\parallel}^2)$ guarantees a smooth transition to $f_i = 0$ for $v_{\parallel} < 0$ and $v_{th} = \sqrt{2k_B T_i/m_i}$ [1].

The coordinate system $(s_x, s_{\perp}, s_{\parallel})$, in which the calculations are performed, is defined by the magnetic field \vec{B} (see Fig. 1), and it is transformed by the equation $v_{xr} = v_x - v_{E \times B}$ to a system moving with the $v_{E \times B} = -E_{\perp}/B$ drift velocity. For the calculations the velocity distribution $f_i(l, \vec{v})$ at the sheath entrance is divided in velocity space into small intervals $d\vec{v}$. In each interval $\vec{v} + d\vec{v}$ a representative particle is chosen, for which the equation of motion $m_i d\vec{v}/dt = ze(\vec{E} + \vec{v} \times \vec{B})$ is numerically solved. The time derivatives of space and velocity coordinates are in the transformed system : $\dot{s}_{\parallel} = v_{\parallel}$; $\dot{s}_{\perp} = v_{\perp}$; $\dot{s}_{xr} = v_{xr}$; $\dot{v}_{\parallel} = ze/m_i E_{\parallel}$;

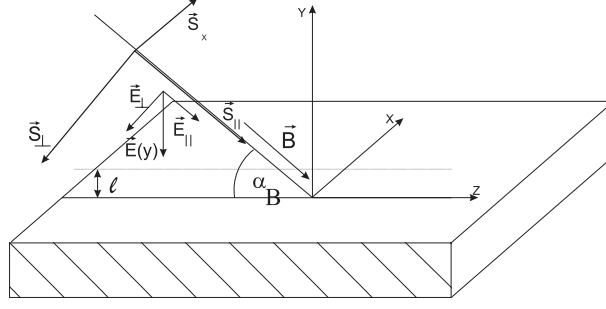


Figure 1. Definition of the coordinate system and the angle of the magnetic field α_B .

$\dot{v}_\perp = \Omega_i v_{xr}$; $\dot{v}_{xr} = -\Omega_i (v_\perp - v_p)$ (gyro-reduced). Here the polarisation drift v_p is described by $v_p = 1/(B\Omega_i) dE_\perp/dt$.

The last equations have the discrete form

$$s_{xr}(t + \Delta t/2) = v_{xr}(t)\Delta t + s_{xr}(t - \Delta t/2);$$

$$v_\perp(t + \Delta t/2) = \Omega_i v_{xr}(t)\Delta t + v_\perp(t - \Delta t/2);$$

$$v_{\parallel}(t + \Delta t/2) = ze/m_i E_{\parallel}(t)\Delta t + v_{\parallel}(t - \Delta t/2); \quad s_\perp(t + \Delta t) = v_\perp(t + \Delta t/2)\Delta t + s_\perp(t);$$

$$s_{\parallel}(t + \Delta t) = v_{\parallel}(t + \Delta t/2)\Delta t + s_{\parallel}(t); \quad y(t + \Delta t) = -s_{\parallel}(t + \Delta t) \sin \alpha_B - s_\perp(t + \Delta t) \cos \alpha_B;$$

$$v_p(t + \Delta t/2) = 1/(\Omega_i B)(E_\perp(t + \Delta t) - E_\perp(t))/\Delta t;$$

$$v_{xr}(t + \Delta t) = -\Omega_i (v_\perp(t + \Delta t/2) - v_p(t + \Delta t/2))\Delta t + v_{xr}(t).$$

The first three equations are shifted with respect to the others by a half time step. This choice opens the opportunity to solve successively the full set of the equations inside the magnetic presheath and Debye sheath. Outside the sheath there exists as a result of the assumption $\vec{E}(y \geq l) = 0$ a simple analytic solution of the equation of motion.

Since there are no sources in the sheath, the fluxes at the sheath entrance and at the wall have to be equal, $\vec{\Gamma}_l = \vec{\Gamma}_w$. It has to be taken into account that at the sheath entrance only the $v_y = v_{\parallel} \sin \alpha_B$ velocity component and at the wall the sum of components $v_{yw} = v_{\parallel w} \sin \alpha_B + v_{\perp w} \cos \alpha_B$ give a contribution. This consideration makes it possible to calculate the velocity distribution of ions at the wall f_w :

$$d^3\Gamma_l = d^3\Gamma_w;$$

$$d^3\Gamma_l = d^3n v_{\parallel} \sin \alpha_B; \quad d^3n = f_l(v_{\parallel}, v_\perp, v_x) dv_{\parallel} dv_\perp dv_x;$$

$$d^3\Gamma_w = d^3n_w (v_{\parallel w} \sin \alpha_B + v_{\perp w} \cos \alpha_B); \quad d^3n_w = f_w(v_{\parallel w}, v_{\perp w}, v_{xw}) dv_{\parallel w} dv_{\perp w} dv_{xw};$$

with $dv_{\parallel w} dv_{\perp w} dv_{xw} = J dv_{\parallel} dv_\perp dv_x$, where J is the Jacobi determinant. From this it follows

$$f_w(v_{\parallel w}, v_{\perp w}, v_{xw}) = f_l(v_{\parallel}, v_\perp, v_x) 1/J(v_{\parallel} \sin \alpha_B) / (v_{\parallel w} \sin \alpha_B + v_{\perp w} \cos \alpha_B).$$

The angle of ion incidence relative to the surface normal is calculated by $\gamma_i = \arccos(-v_{yw}/|\vec{v}_w|)$, and the average value of this angle is given by

$$\langle \gamma_i \rangle = \int \gamma_i f_w(v_{\parallel w}, v_{\perp w}, v_{xw}) dv_{\parallel w} dv_{\perp w} dv_{xw} / \int f_w(v_{\parallel w}, v_{\perp w}, v_{xw}) dv_{\parallel w} dv_{\perp w} dv_{xw}.$$

3. Results and Discussion

The velocity distribution of Helium ions at the magnetic presheath entrance is illustrated in the (v_\perp, v_x) - gyro-plane in Fig. 2 a). For the calculations of the velocity distribution of impurity ions the same potential was used as in Ref. [1]. The plasma parameters are $\alpha_B = 6^\circ$, $T_e = 20eV$, $T_i/T_e=1$, $n_e = 10^{12} cm^{-3}$ and $B = 2$ Tesla. Fig. 2 b) shows the the velocity distribution of

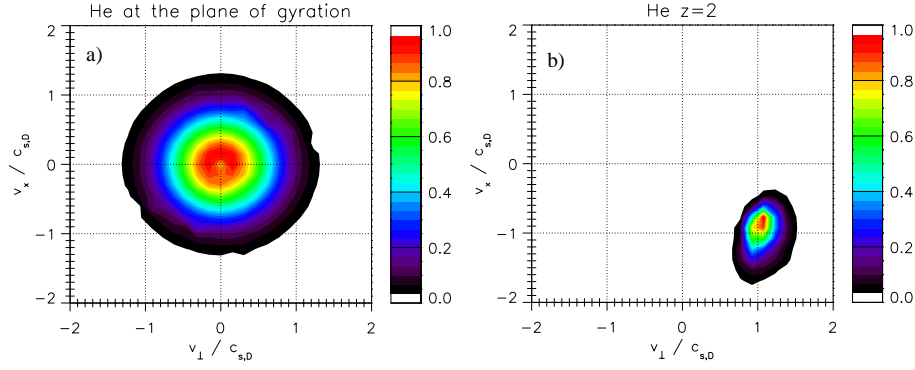


Figure 2. Velocity distribution in the plane of gyration at the magnetic sheath entrance a) and at the wall b).

He^{2+} at the wall in the (v_{\perp}, v_x) - gyro-plane. Two effects were observed: First a shift of the maximum of the velocity distribution as a result of the $v_{E \times B}$ drift and the polarisation drift. Second gyrocooling effect (first described in [2]) whereby the thermal energy of gyro-motion is gradually converted into kinetic energy of drift motion (the velocity distribution at the wall is “squeezed”). The influence of the mass on the velocity distribution is shown in Figs. 2 b), 3 a) and 3 b), where the maximum is shifted from $(v_{\perp}, v_x)/c_{s,D} = (1.1, -0.9)$ in 2 b) to $(v_{\perp}, v_x)/c_{s,D} = (0.7, -0.4)$ in 3 a) and to $(v_{\perp}, v_x)/c_{s,D} = (0.6, -0.2)$ in 3 b). The different widths of the velocity distribution are due to the different thermal velocities $v_{th} \sim 1/\sqrt{m_i}$. The influence of the charge on the velocity distribution is shown in Figs. 3 a), c) and d). For highly charged ions the drifts are larger than for lowly charged ions.

A potential of a double exponential form with a dependency on the magnetic field angle is used[4] to calculate the average angle of incidence of the ions at the wall. Fig. 3 e) illustrates the average angle of incidence of hydrogen ions. The application of our model on hydrogen ions shows a good agreement with the results as obtained in [3]. The differences have their cause in a different potential and in a different velocity distribution at the entrance of the magnetic presheath. The average angles of incidence are shown in Fig. 3 f) for different impurity ions. For a shallow magnetic field angle α_B the drifts of the light ions (He^{2+}) are larger than for the heavy ions (Ne^{2+}). This is the reason why $\gamma_{He^{2+}} < \gamma_{Ne^{2+}}$. For a perpendicular magnetic field, however the width of the velocity distribution, which depends on $v_{th} \sim 1/\sqrt{m_i}$, dominates the average angle of incidence leading to $\gamma_{He^{2+}} > \gamma_{Ne^{2+}}$.

It should be noticed that our model is based on the possibility to calculate single ion orbits. The comparison in ref. [5] of the Deuterium ion orbits in a linearly increasing electrical field with ref. [2] shows an excellent agreement. The velocity distributions for Deuterium ions which are published in ref. [1] could also be reproduced [5]. At least 10^4 ions must be followed in order to reduce the statistical error sufficiently for getting smooth profiles.

In the present paper it has been shown that with our model we are now able to calculate also the average angle of incidence of impurity ions which is a sensitive parameter for plasma wall interaction. Additionally we displayed with the model the influence of the $v_{E \times B}$ drift and the polarisation drift on the angle of incidence.

References

- [1] H. Gerhauser, H.A. Claaßen: Contrib. Plasma Phys. **38**(1/2), 331-336 (1998)
- [2] H.A. Claaßen, H. Gerhauser: Contrib. Plasma Phys. **36**(2/3), 381-385 (1996)

- [3] R. Chodura: J. Nucl. Mat. **111-112**, 420-423 (1982)
 [4] J.N. Brooks: Phys. Fluids B **2** (8),1858-1863 (1990)
 [5] P. Lindner: “Untersuchung der Freisetzungsmechanismen von Helium und Neon an Kohlenstoff und Wolfram in TEXTOR-94.” Thesis at Heinrich-Heine-Universität Düsseldorf (1998)

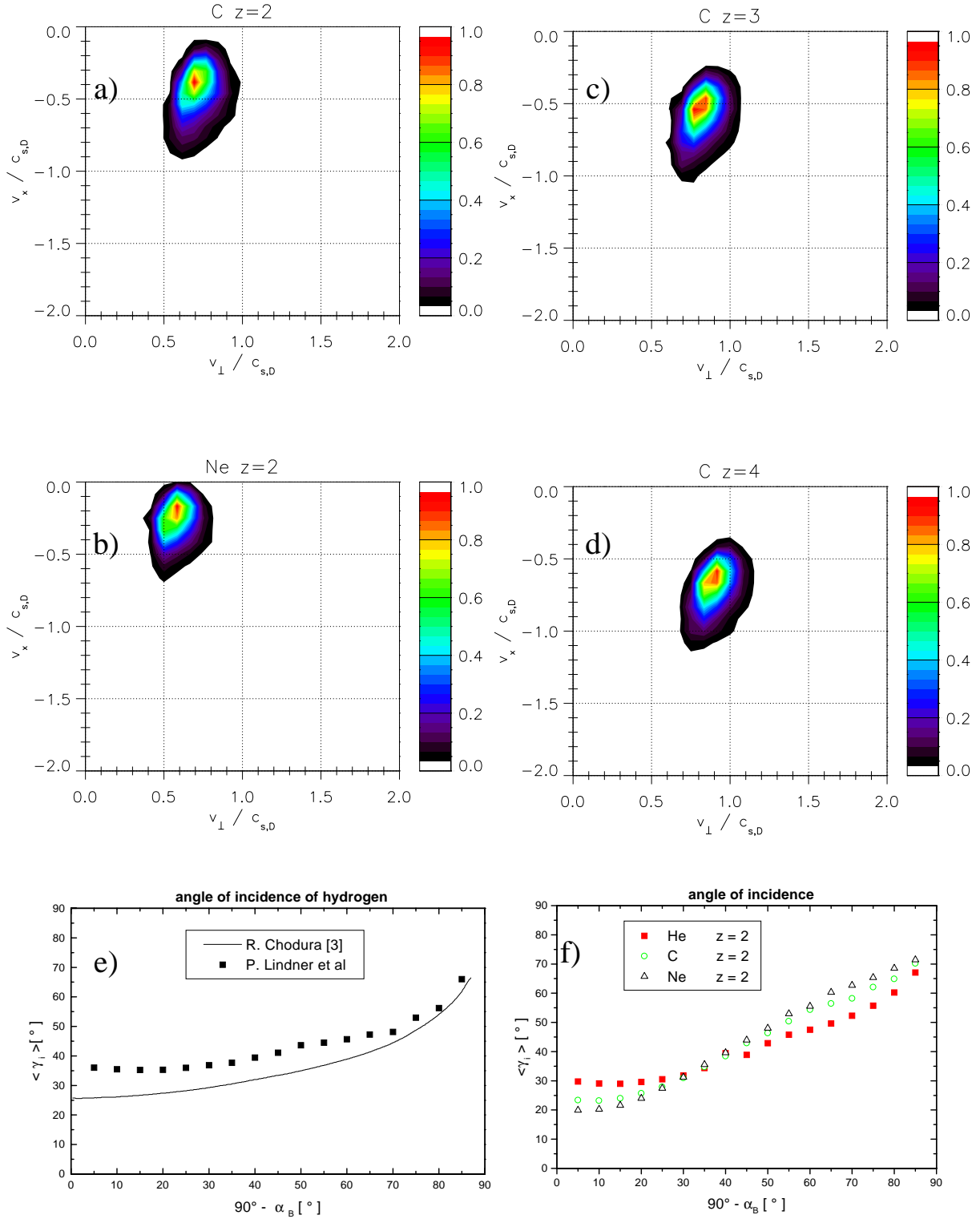


Figure 3. Velocity distribution in the plane of gyration at the wall a), b), c), d) and the average angle of incidence for different species e), f). The plasma parameters for f) are $T_e = 30eV$, $T_i/T_e = 2$, $n_e = 5 \cdot 10^{12} cm^{-3}$ and $B = 2.25$ Tesla.